ARTICLES

Different regimes of light localization in a disordered photonic crystal

Yu. A. Vlasov,* M. A. Kaliteevski,† and V. V. Nikolaev
A. F. Ioffe Physical-Technical Institute, 194021 St. Petersburg, Russia
(Received 2 December 1998)

It is known that photonic Bloch states can become strongly localized near the band edges in a disordered photonic crystal. We show that Bloch states are disrupted and another localization regime establishes when local fluctuations of the band-edge frequency caused by randomization of refractive index profile becomes as large as the band-gap width. Transmission experiments performed on opal photonic crystal have shown the exponential decay of light throughout the gap region, which is ascribed to building up of the second regime of light localization. [S0163-1829(99)11027-0]

I. INTRODUCTION

Light localization in disordered media[1–4] can be caused when constructive interference of backscattered waves brings transport to a complete halt (strong or Anderson localization). In this regime the transport mean free path l becomes as short as the wavelength of the wave λ and the Ioffe-Regel (IR) criterion for localization $kl<1$ is satisfied,[5] where $k=2\pi/\lambda$. During the last decades there has been a considerable interest in experimental verification of light localization.[2–4] In this context it was first suggested by S. John[6] that the IR criterion can be more easily satisfied in periodic dielectric structures. The density of photonic states (DOS) in the band gap of such a photonic crystal can be suppressed to zero giving rise to omnidirectional photonic band gap (PBG).[7] It was argued[6] that in a photonic crystal, in which some disorder is introduced, the wave vector k in the IR criterion should be replaced by the ''crystal momentum'' k_{cryst} when the frequency of the wave is near a photonic band edge of the average periodic structure. Even for a very weak disorder (large mean free path l) $k_{cryst}l$ can become smaller than unity for some frequency range at the zone boundary, where k_{cryst} goes to zero. Since first being introduced, this approach has not been tested experimentally except in recent studies of microwave transmission in a three-dimensional (3D) periodic structure with disorder.[8]

Another motivation for such studies comes from important technological applications, which can be developed on the basis of photonic crystals.[7] The faults and defects occurring during production stage can, however, quickly destroy the required uniformity and regularity of the photonic lattice and thus smear out the desired effects of decreased DOS because of the filling of PBG by bandtail localized states.

In this paper we present the results of theoretical analysis and experimental studies aimed at the investigation of the ''subtle interplay of order and disorder''[6] in a disturbed 3D photonic crystal, which is required for observation of Anderson localization of photons. As a model system we chose synthetic opals,[9–18] which are composed of nearly monodisperse (standard deviation δ about 5%) submicron silica spheres, closely packed in a face-centered-cubic (fcc) lattice with a period of $\approx$200 nm. It has already been demonstrated that opals possess photonic gaps throughout the visible spectrum.[9,10] It was predicted that it is technologically possible to achieve in opals small but complete PBG extending throughout the whole Brillouin zone (BZ).[11,14] These predictions stimulate intense experimental studies of various routes for fabrication of so-called ''inverted opals'' (refractive index of the interstitials n_b is larger than that of the spheres n_a), in which the silica periodic lattice is used as a scaffolding for high refractive index material as titania,[15] graphite,[16] or semiconductor quantum dots.[17] After removing of the silica spheres from the structure the refractive index contrast can be increased to extremely high values, sufficient for opening up of a complete PBG. Even for inverted opal with not as high refractive index contrast of only 2 an enhancement of optical gain by a factor of 3 and appearance of lasing was reported recently.[12]

The paper is organized as follows. Section II describes samples preparation and experimental setup. In Sec. III we present the results of transmission measurements. Section IV is devoted to results of theoretical calculations of transmission in perfectly ordered and in randomly disordered photonic crystal. We introduce two different regimes of light localization in disordered photonic crystal in Sec. V. In Sec. VI we discuss the obtained results.

II. EXPERIMENT

The sample of synthetic opal used in this study was fabricated by three subsequent technological procedures. At first the monodisperse suspension of SiO_2 spheres with mean diameter of $d=197$ nm was synthesized by Stöber method.[19] Dynamic light-scattering and scanning electron microscopy (SEM) measurements show that the standard deviation δ of the spheres diameter is less than 5%. The spheres settle down on a flat quartz substrate and self-organize in a three-dimensionally periodic structure. Our previous studies[10,13] have shown that the resulting samples possess highly ordered fcc structure with some conventional lattice defects like

stacking faults, dislocations, etc. The average concentration of point defects was estimated by SEM to be of the order of 1 defect per 100 unit cells. The concentration of stacking faults is found to be 20%.[13] Finally the ordered sediment is annealed at hydrothermal conditions in autoclave to provide hardness and to obtain self-supporting solid samples with dimensions in a cm range. The lattice constant of the sample under study is found by SEM to be $a=276$ nm, which implies the volume packing fraction of the spheres $\beta=0.76$ slightly larger than close packed as a result of sintering. These parameters define the position of a photonic gap along the [111] direction to be centered at a wavelengths around 460 nm.[11]

In order to study different mechanisms, responsible for light attenuation in synthetic opals, we measure transmission as a function of a sample thickness. This method is widely used in studies of photon transport in disordered media.[2,4] For this purpose the opal sample with lateral dimensions of 6×3 mm and thickness 350 μm was polished to a form of a wedge of 0.050 rad with a base corresponding to a (111) crystallographic plane of a fcc lattice of synthetic opal. L linearly increases with distance along the base direction changing from about 50 to 350 μm, or from about 300 to 1900 parallel (111) planes, thus allowing a scan of L by exact positioning of the sample on a computer controlled translational stage. The probing light beam is incident normal to a (111) base plane.

III. RESULTS

A. Total transmission

Two types of experiments were performed in a wedged sample. In a first set of experiments the total transmission is measured. The inset in Fig. 1 shows the corresponding experimental setup. The spatially filtered and collimated laser beam is used as a light source. It is projected on a sample in a form of a narrow, 100-μm wide stripe oriented along direction perpendicular to the long 6-mm base of the sample. This allows us to average the transmission signal over the whole 3-mm width of the sample and to obtain smooth attenuation curves. The sample moves slowly along its long direction with respect to a fixed diaphragm D_1. The refractive index contrast of our wedged sample, which is defined by the ratio of refractive index of silica spheres ($n_a=1.37$) and that of air in the interstitials ($n_b=1$), is relatively high. As a result, light is exiting the sample at large thicknesses as a diffuse, very broad beam. Transmitted light is passed through a diffuser P and is collected by a photodiode PD placed immediately after the sample in front of a diaphragm. Thus all ballistic light as well as all light diffusely scattered in a forward direction is collected.

Figure 1 represents the total attenuation curves measured as a function of a sample thickness. Attenuation curve in Fig. 1(a) is measured at wavelength of a He-Ne laser 632.8 nm, far to the red from the position of a [111]-photonic gap (460 nm). The sample starts at about 40 μm and the first large drop in transmission can be ascribed to scattering on the surface. Relatively slow decrease of transmission at larger thickness corresponds to scattering in the bulk of the sample. It can be seen that in this region the attenuation curve in Fig. 1(a) can be well fitted by inverse dependence $T=l/L$, characteristic of a classical diffusion.[1,2,4] The mean free path l can be estimated from the slope as 20 μm. This gives the estimate for $kl\approx250$. This value is in accordance with data reported for a sample made of silica beads with comparable mean diameter and packing fraction.[20] At a very large sample thickness ($L>300$ μm) the experimental curve exhibits smaller transmission than expected from inverse law indicating the onset of absorption. The absorption decay length L_a taken as 350 μm can be used for estimation of an absorption length $l_a=1.8$ cm (inverse absorption coefficient α) according to Boltzmann diffusion relation $l_a=3L_a^2/l$. This gives an absorption coefficient of only $\alpha=0.5$ cm^{-1}.

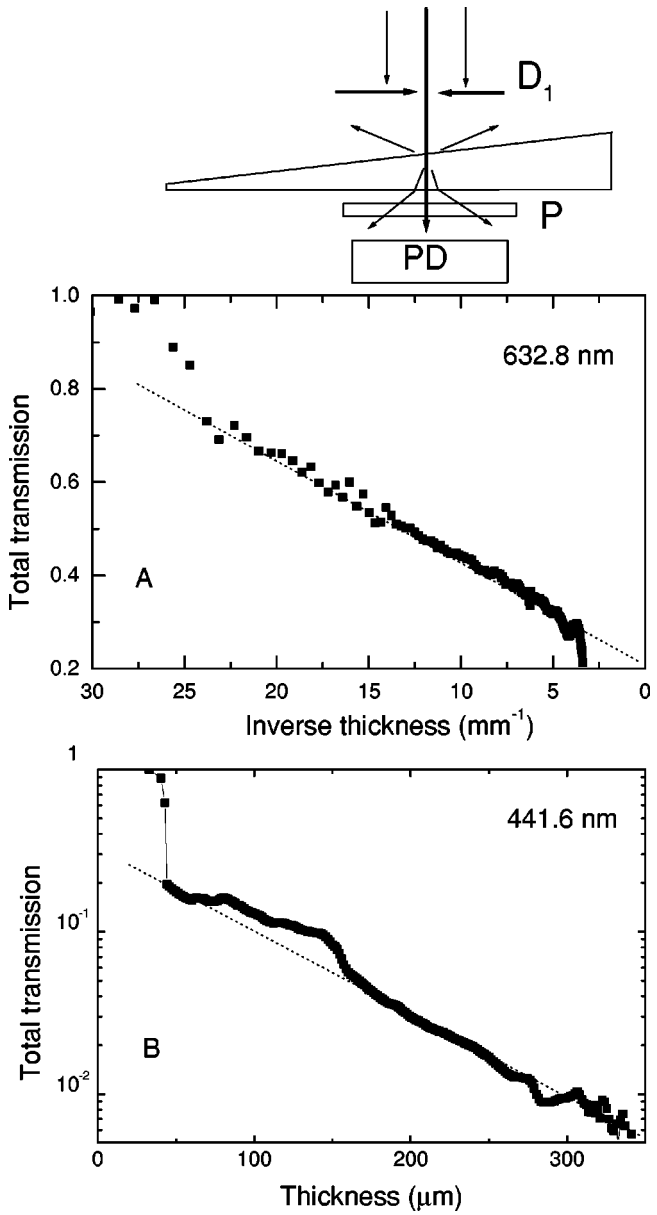

FIG. 1. Experimental normalized total transmission of an opal sample with $n_a/n_b=1.37$ measured at two wavelengths of (a) 632.8 nm and (b) 441.6 nm. In (a) thicknesses are plotted in inverse scale. Dotted line is classical diffusion dependence $T=l/L$ with $l=20$ μm. In (b) data are presented on a semilogarithmic scale. The solid line is an exponential fit $\exp(-L/\xi)$ with $\xi=90$ cm^{-1}. Inset: Sketch of experimental setup for total transmission measurements on a wedged sample. D_1: diaphragm; P: diffuser; PD: photodiode.

The attenuation curve presented in Fig. 1(b) is measured at a wavelength of a He-Cd laser 441.6 nm, close to the position of a [111] photonic gap. It is plotted on a semilogarithmic scale and exhibits a strikingly different exponential fall of transmission with thickness with attenuation length ξ of about 90 cm^{-1}. Three main mechanisms can be considered for explanation of the exponential decay of light intensity with thickness in a periodic photonic crystal with disorder—absorption, Bragg diffraction, and Anderson localization. It is very hard to believe, however, that a refractive index contrast of only 1.37 can cause Anderson localization. For estimation of absorption at the 441.6-nm wavelength of interest we measure total attenuation in a wedged sample immersed in index matched mixture of glycerol and water ($n_a = n_b$). The thickness dependence is found to be very weak and is mainly governed by a residual scattering on the surfaces. Estimate of the absorption coefficient gives the upper value of 1 cm^{-1}. According to Rayleigh dependence the mean free path l can be decreased from 20 μm at 632.8 nm to 10 μm ($kl = 125$) at 441.6 nm. It is unlikely, however, that it falls as low as 3.7 μm ($kl = 46$)—the value which can explain observed exponential attenuation $\xi = 90$ cm^{-1}. In the latter case, in contradiction with experimental curve, the initial inverse dependence should be observable at thicknesses smaller than $L_a = 100$ μm. Therefore the most likely explanation of the observed exponential attenuation is Bragg diffraction on a periodic structure.

B. Zero-order transmission

In order to distinguish between various mechanisms of light attenuation we perform spectrally resolved experiments. To decrease significantly the incoherent scattering on sample surfaces the wedged sample was immersed in a glycerin thus implying the refractive index of the interstitials to be $n_b = 1.47$. In this situation the pattern of transmitted light is mainly composed of zero-order ballistically transmitted beam surrounded by a weak diffuse halo. In this second set of experiments transmission spectra of only a zero-order ballistic transmitted light is studied as a function of a sample thickness. This is performed by the use of a setup shown in the inset of Fig. 2 and described in details in Ref. 11. The incident white light beam is produced from an incandescent lamp. In order to minimize the contribution of the spurious diffusely scattered background to the detected signal, the incident beam was highly collimated (divergence less than 200 mrad). The sample is illuminated through a fixed 100-μm diameter diaphragm D_1 placed immediately before the sample, thus defining the probing area. Transmitted light is collected in the direction of incidence within a very narrow angular cone defined by a second diaphragm D_2, which transmits a zero-order beam only. This light is then dispersed with a double, 1.5-m base monochromator (0.5-nm spectral resolution) and recorded by a photomultiplier.

Figure 2 presents a set of transmission spectra taken from the wedged sample filled with glycerin exhibiting the strongly attenuated band at 460 nm. This dip is accompanied by an intense line in reflection spectrum with reflectivity close to unity, which repeats the shape and spectral position of the dip in transmission.[9,10,13] This band can be ascribed to coherent Bragg scattering on parallel set of (111) planes of

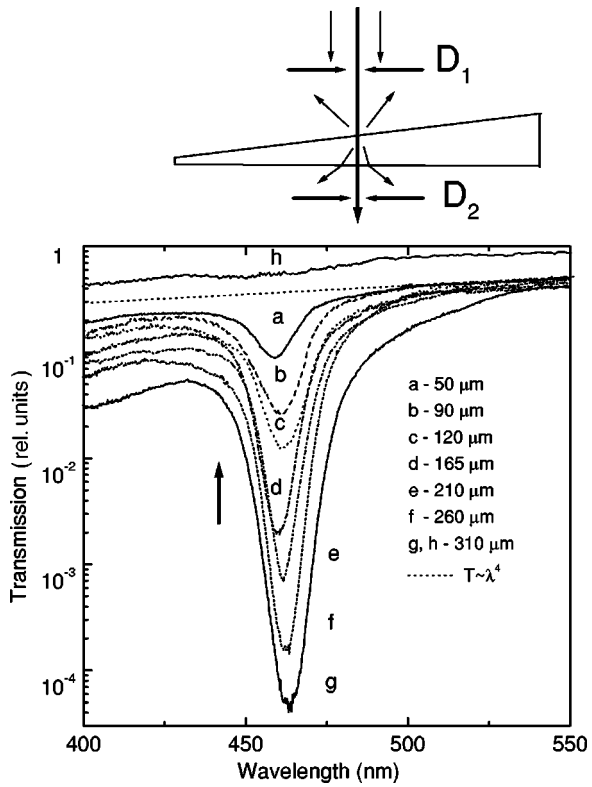

FIG. 2. Experimental zero-order transmission spectra of the wedged sample with $n_b = 1.475$ measured as a function of the sample thickness L. The magnitude of attenuation in all of the spectra were normalized to unity at $\lambda = 900$ nm, where the sample can be assumed to be completely transparent. Spectra a–g correspond to different thickness from 50–310 μm. Curve h represents the spectrum for 310-μm thickness in index-matched glycerol/water mixture with $n_b = 1.37$. The dotted curve gives the dependence $T \propto \lambda^4$. Arrows indicate a wavelength of 441.6 nm for which the total transmission in Fig. 1(b) is measured. Inset: Sketch of experimental setup for measurements of zero-order transmission on a wedged sample. D_1, D_2: diaphragms.

the crystal and can be referred to as a [111]-photonic gap. The attenuation at the center of the gap strongly increases by 4 orders of magnitude while the position of the probe light beam is changed along the wedge direction (i.e., while the thickness of the sample L is increased). A smooth decline in transmission spectra to shorter wavelengths can be attributed to incoherent scattering from lattice imperfections and impurities. In the long-wavelength region ($\lambda > 550$ nm) it can be approximated by the characteristic Rayleigh powerlike dependence (see dotted curve $T \sim \lambda^4$ in Fig. 2). The magnitude of attenuation in all of the spectra were normalized to unity on the long-wavelength limit ($\lambda = 900$ nm), where the samples can be assumed to be completely transparent. From Fig. 2 it can be seen also that the spectral position of the gap remains practically unchanged throughout the sample—the deviations of the central wavelengths from the mean value of 460 nm are not larger than 5 nm. It means that the crystal preserves the same periodicity on average at least along the 6-mm probe direction. Therefore the central gap frequency expressed in units of $c/\langle a \rangle$, where c-speed of light, $\langle a \rangle$-mean lattice constant, can be assumed to be constant throughout the crystal as $\nu_0 = 0.60$ and the deviations of the

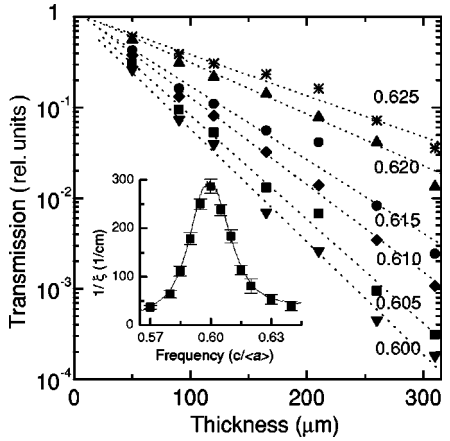

FIG. 3. Experimental thickness dependencies of zero-order attenuation for frequencies $\nu=0.605$–0.625. Dotted lines are least-square exponential fits to the experimental data. Inset: Inverse attenuation length $1/\xi$ obtained by fitting of attenuation curves for frequencies within the gap region. Solid line is the experimental transmission spectrum $-\ln(T)$ divided by the sample thickness.

gap position are caused by the deviations of the mean lattice constant about 1%. Thus the central gap frequency in each of the spectra can be corrected to have the same frequency $\nu_0=0.60$.

Figure 3 depicts the values of attenuation $T(L)$ (Rayleigh contribution is already subtracted[11]) for frequencies near the upper band edge at $\nu=0.600$–0.625, which exhibit exponential decay slowing down toward the band edge. The inset in Fig. 4 represents the inverse attenuation length $1/\xi$ obtained by exponential fitting of each of the $T(L)$ curves for all the frequencies from $\nu=0.55$–0.65 covering all the gap region. The logarithm of transmission spectrum for $L=210$ μm divided by the sample thickness $\ln(T)/L$ is also plotted for comparison. It is seen that the transmission spectrum closely coincides with measured values of inverse attenuation length, which means that attenuation remains exponential throughout the gap region.

In order to check possible contribution of absorption to observed attenuation, we analyze transmission of the sample immersed in index matched glycerin/water mixture ($n_a \approx n_b$). The corresponding spectrum h in Fig. 2 exhibits the absence of the photonic gap related dip. Weak attenuation remaining at the wavelengths of interest can be attributed to scattering on the surfaces as well as to a very small residual absorption, an upper limit of which can be estimated to be not larger than 1 cm^{-1} close to a value obtained in total transmission measurements. Further analysis of the interplay between the remaining two mechanisms—Bragg diffraction and incoherent scattering on defects—requires comparison of experimental measurements with numerical calculations.

IV. THEORY

A. Transmission in a perfectly periodic system

For numerical simulations we use the routine one-dimensional transfer-matrix method,[21–23] in which experimental 3D fcc structure is modeled by a refractive index profile, which is periodic only in the [111] direction. In order to incorporate the actual experimental parameters of the system into the calculation scheme (spheres diameter d and volume packing fraction β) the profile is calculated as

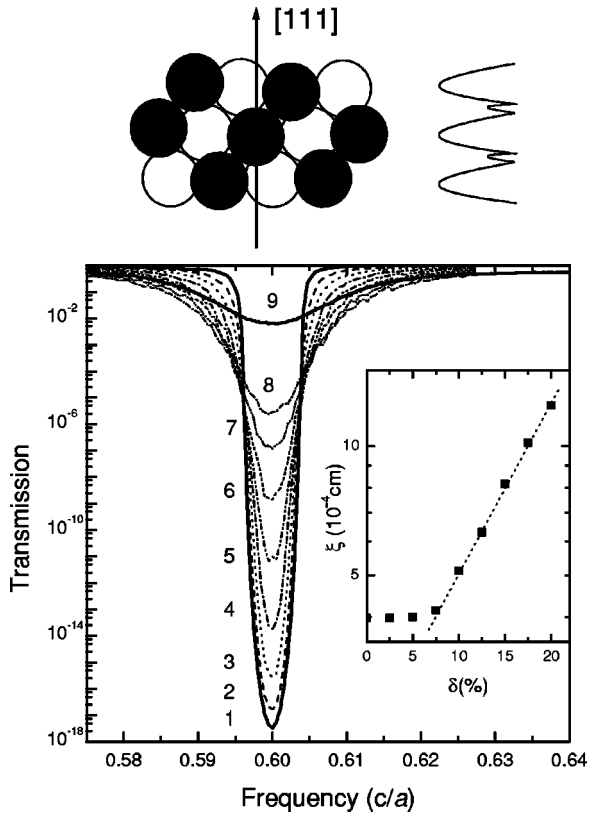

FIG. 4. Calculated transmission spectra for photonic crystal of 165-μm thickness with varying disorder, each ensemble averaged over 200 realizations. The standard deviation δ of the spheres diameter is 1–0 %, 2–0.5 %, 3–1 %, 4–2 %, 5–3 %, 6–4 %, 7–5 %, 8–10 %. Thick solid line 9 is the experimental spectrum. Upper inset: Scheme of spheres packaging on a (110) plane of a fcc lattice of opal and corresponding profile of refractive index calculated along the [111] direction. Lower inset: A semilogarithmic plot of calculated attenuation length ξ as a function of disorder δ.

$$n(z)=S_{sp}(z)n_a+[1-S_{sp}(z)]n_b, \tag{1}$$

where $S_{sp}(z)$ is relative area cross section of the spheres in a (111) plane calculated as a function of the distance along the [111] z direction. The calculated analytical expression for this profile, which is shown in the inset of Fig. 4, can be found in the Appendix. Refractive indices of the spheres ($n_a=1.37$) and surrounding media ($n_b=1.47$) are chosen close to experimental values. The calculated transmission spectrum of an ideal periodic structure of a thickness of 165 μm is presented in Fig. 4, curve 1. It exhibits a gap centered at reduced frequency $\nu_0=0.60$ (in units of c/a, where c is the speed of light, a is the fcc lattice constant). Its relative width $\Delta\nu/\nu_0$ is about 1% with a midgap value of imaginary wave vector $\mathrm{Im}(\mathbf{k})$ of 1300 cm^{-1}.

Comparison of experimentally measured quantities of interest ($1/\xi$ and $\Delta\nu/\nu_0$) with that calculated for perfect periodic structure shows that $1/\xi$ is about four times smaller, while the width $\Delta\nu/\nu_0$ is at least seven times larger in the experimental sample. These discrepancies become obvious from a comparison of the corresponding calculated (curve 1) and experimental (curve 9) transmission spectra presented in

Fig. 4 for the sample of 165-μm thickness. It is clearly seen that at the gap central frequency $\nu_0 = 0.60$ the transmission in the experimental sample is more than 15 orders of magnitude larger, while at the band edges it is smaller. Note that experimental geometry used allows one to measure gaps down to 6 orders of magnitude deep (-60 dB). Therefore increased transmission at the gap center cannot be explained by the contribution from stray scattered background. Neither can it be attributed to the shortcuts of the model used. It should be noted that, even if our model is one-dimensional and scalar, the results for the [111] gap appear to be in a fairly good quantitative agreement with calculations employing a full-vector 3D approach.[24] Note that for fcc lattice it is the [111] closed packed layers which give the dominant contribution to diffraction, especially in the case of relatively low refractive index contrast. This can explain good quantitative agreement of the results obtained by our 1D model and full-vector 3D calculations.[24] We should emphasize that this remarkable and unexpected difference between the calculated and experimentally measured attenuation length and width of the photonic gap is one of the main results of our experimental studies. It indicates the strong influence of disorder on transport properties of opal photonic crystal.

We should return at this point once again to a discussion of possible contribution of absorption to experimentally observed exponential attenuation. Even the absorption coefficient, as it was shown above, is rather small; effective absorption can be large due to the increase of a dwell time of light inside the structure. The time of flight of photons has been measured recently on analogous opal sample at the band-gap frequencies.[18] It has been found that propagation delay of femtosecond light pulses is 1.3–1.5 times longer due to multiple scattering and/or group velocity dispersion at the edges of a photonic gap.[18] It should be noted, however, that experimentally observed transmission at the midgap, which is considerably *larger* than expected for perfectly periodic structure, strongly contradicts to possible assignment of observed exponential attenuation to contribution of absorption. Indeed, the role of inelastic scattering, especially increased absorption due to increase of the dwell time, could result only in further *decrease* of transmission at the midgap from the value characteristic of a periodic structure. Thus experimentally observed exponential decay is attributed solely to elastic scattering.

B. Transmission in a disordered periodic-on-average structure

So this is more likely the combination of coherent Bragg diffraction and incoherent scattering, which is responsible for the observed behavior. In order to obtain some qualitative insight in the problem we perform calculations of transmission spectra of a disordered photonic crystal. The disorder is incorporated in the model in analogy with the experimental case of opals by a random distribution of the spheres diameters δ, which was chosen to be flat for simplicity. Figure 4 represents a set of transmission spectra (curves 2–8), each averaged over 200 random configurations, calculated for different values of disorder. Note that presence of disorder leads to exponential decay of light with thickness not only within the former gap of the periodic structure (curve 1), but also in the former passbands, thus significantly broadening the gap. The attenuation length ξ is usually defined as

$$\xi^{-1} = -\frac{\langle \ln T \rangle}{L}, \tag{2}$$

where L is the sample thickness and brackets denote the ensemble averaging over various (in general, infinite) different random configurations.[22,23,21] The general tendency for increased transmission at the midgap and decreased at the band edges, already pointed out in the references,[8,22,23,21] is clearly seen. It is commonly believed that this counterintuitive effect (increasing transmission with increase of disorder) is the result of the increased photonic DOS due to appearance of strongly localized photonic bandtail states, which fill the gap.[22,21,23] In this context ξ defined by Eq. (1) is often called ''localization length.''[21–23] The inset in Fig. 4 represents ξ calculated for the gap center as a function of disorder δ and plotted in a semilogarithmic scale. It can be seen that ξ increases exponentially with increase of disorder at high enough δ. Such behavior is just what is expected for the increased DOS of localized states. In what follows, however, we will present an alternative analysis of light localization in a disturbed periodic structure.

V. DIFFERENT REGIMES OF LIGHT LOCALIZATION

We believe that, depending on the amount of disorder δ, at least two qualitatively different localization regimes build up consequently. Indeed, any type of random error in periodic lattice is equivalent to adding (subtracting) some dielectric material from the unit cell of an average periodic system. This results in increase (decrease) of an average dielectric constant and consequently in a disorder induced local shift of the band edge $\Delta\nu_0$, which can exceed for large enough δ the normalized gap width $\Delta\nu/\nu_0$. In the case $\Delta\nu_0 \ll \Delta\nu/\nu_0$ the waves at the band edges can be well described by the wave vector k_{cryst} of the average periodic structure. For large enough disorder, however, the shift of the band edges $\Delta\nu_0$ can exceed the width of the gap itself $\Delta\nu/\nu_0$. In this regime the terms ''band structure of the periodic-on-average system'' as well as k_{cryst} lose their meaning. Increase of transmission in the gap region does not already reflect the increase of the density of localized bandtail states, because the passband states also become involved in transmission.

A. First localization regime: $\delta \ll \Delta\nu/\nu_0$

This general idea becomes quite clear for the model opal system under investigation. Indeed in opals the deviation δ of the spheres diameter d results in a local deviation of fcc lattice constant $a = \sqrt{2}\cdot d$ and in a corresponding local fluctuation of the photonic band-edge frequency. This forms a random profile of refractive index on which the Bloch wave is scattered. In the case $\delta \ll \Delta\nu/\nu_0$ the waves at the band edges can be well described by the wave vector of the average periodic structure and the modified IR criterion[6] can be applied for the analysis of localization. Figure 5 shows the lower envelope of the square of electric-field amplitude inside the opal structure calculated for the frequency $\nu_0 = 0.596$ in the passband near the conduction-band edge for different values of disorder δ. Note that the profiles pre-

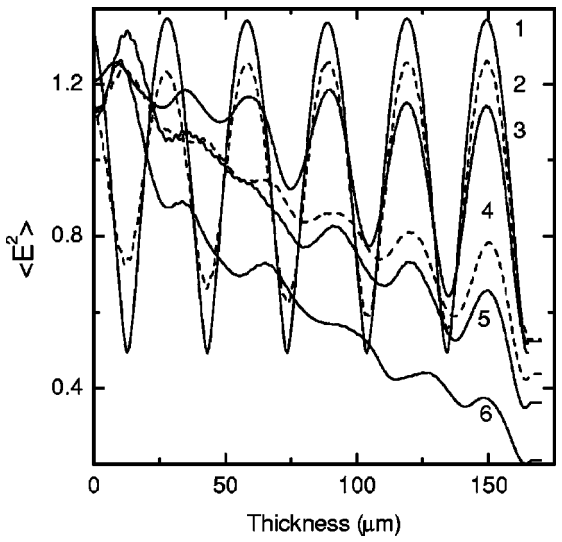

FIG. 5. Calculated low-frequency envelopes of electric-field intensity profiles for the frequency $\nu_0=0.596$ averaged over 200 random configurations. The standard deviation δ of the spheres diameter is 1–0 %, 2–0.5 %, 3–1 %, 4–3 %, 5–4 %, 6–6 %.

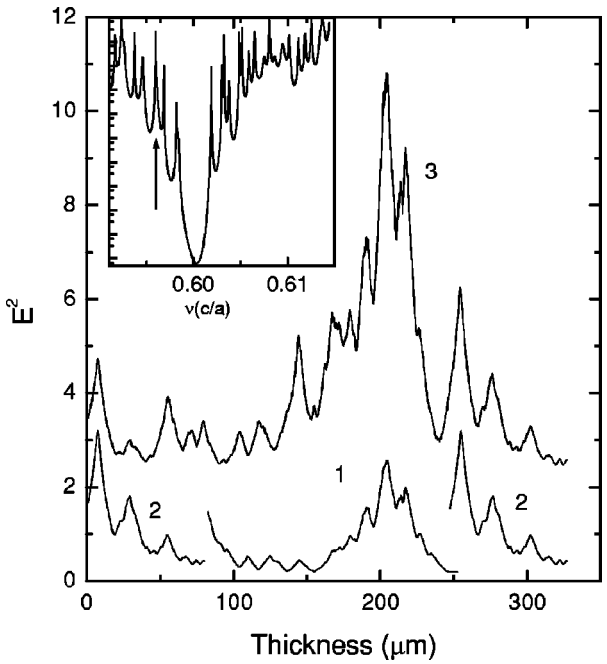

FIG. 6. Calculated low-frequency envelopes of electric-field intensity profiles for the frequency $\nu_0=0.596$ for a single configuration of disorder of $\delta=20\%$. Configuration is chosen the same as that used for calculation of transmission spectrum in the inset. Curve 1 corresponds to the structure of 165-μm thickness, while curves 2 correspond to 82.5 μm. Curve 3 corresponds to the structure of 330-μm thickness combined from the structure 1 at the center and two structures 2 stacked to it from both sides. Inset: Transmission spectrum for a single realization of $\delta=20\%$ disorder in the structure plotted in a semilogarithmic scale. The arrow shows the frequency $\nu=0.596$ of the localized mode for which profiles in the main figure are calculated.

sented are averaged over 200 random configurations thus reflecting the band structure of the averaged periodic system. It is seen that in a perfect periodic structure ($\delta=0$), the wave is nearly a standing at a given frequency (curve 1). The corresponding periodic envelope function is defined by $k_{cryst}=1.9\times10^5$ cm^{-1}. The incorporation of disorder leads to a rapid destruction of coherence (note the vanishing amplitude of the low-frequency periodic modulation in curves 2–5). Low-frequency periodic envelope still exists, however, for some value of disorder, which means that the modified IR criterion[6] $k_{cryst}l<1$ can still be applied. Note that l corresponds now to the mean free path in which this coherent Bloch state is disrupted. For example, $\delta=0.5\%$ for curve 2 and the corresponding l can be estimated to be 10^{-3} cm, which gives $k_{cryst}l\approx100$. As the frequency approaches the band edge, k_{cryst} approaches zero. Therefore for a 1D crystal there always exists such a frequency region close to the band edge where $k_{cryst}l<1$. In order to obtain strong spatial localization in a 3D periodic structure, it is necessary to achieve energy coincidence of such localization regions at the band edges for all the directions, which is the condition reminiscent of that for opening up of the omnidirectional PBG.[7] Note that this regime has a direct analogy with the concepts of electron localization in disordered semiconductors. For example, in the theory of mixed semiconductor crystals[25] the characteristic energy E_0, which defines the width of the tail of localized states, is counted from the former band edge of corresponding perfect crystal and therefore represents the same k_{cryst}.

B. Second localization regime: $\delta\geqslant\Delta\nu/\nu_0$

A qualitatively different regime builds up when $\delta\geqslant\Delta\nu/\nu_0$. The local fluctuations of the band-edge frequency are so large that they exceed the whole width of the gap. In this case the terms usually used in photonic band-gap studies as ''band edges,'' ''band structure,'' etc. lose their meaning completely. Therefore the modified IR criterion[6] cannot be applied for analysis of such a situation. It is, for example, a solid alloy of ultra-narrow-gap semiconductor that can be considered as an electronic analogy of this situation.

We can argue, however, that this regime also differed strongly from light diffusion or localization in completely disordered media, if disorder is not extremely large (the structure can still be considered periodic on average). The photon transport in this case is strongly modified by the presence of periodic potential, even if the latter is strongly disturbed by randomness. For frequencies in the former passbands, a nonzero probability appears for finding large, sufficiently ordered regions, which act as, even disordered, Bragg mirrors (frequencies fall in the gap). As a result, exponential attenuation of the wave appears in configurationally averaged amplitude profiles (see curves 4–6 in Fig. 5) even at frequencies in the former passband of periodic structure. Apart from smooth ensemble-averaged transmission spectra in Fig. 4 the sharp resonant modes appear for a single realization of disorder. The inset in Fig. 6 represents the spectrum of a 165-μm-thick sample calculated for a single realization of $\delta=20\%$ disorder. Sharp defect modes characterized by a large Q factor and transmission close to unity are clearly seen. Figure 6 displays the squared electric-field profiles inside this structure for frequency corresponding to one of such resonant modes at $\nu_0=0.596$ in the former passband (see arrow in the inset of Fig. 6). It can be seen that these resonant states are characterized by a huge enhancement of

electric-field amplitude and appearance of exponential tails due to destructive Bragg interference in ordered-on-average regions.

Thus these states resemble the well-known from textbooks form of localized states. It should be noted that such states cannot be described by ''localization'' considered in the theory of wave propagation in disordered media.[1–4,20] Neither is it, however, the localization in periodic structure for which the modified IR criterion is valid.[6] Thus it is some different regime of, let us say, ''spatial confinement'' of the wave caused by coherent back reflection. It is the Thouless criterion of localization[26] which we use to examine such spatially confined states. It requires essentially that the width of energy levels be smaller than the energy spacing between them in order to prevent tunneling between states and to block the transport. We calculate the field profile for a single realization of disorder in a 165-μm thickness sample (see curve 1 in Fig. 6). The realization is chosen the same as for spectrum in the inset of Fig. 6 for frequency $\nu_0 = 0.596$, for which the resonant state exists. The resulting field profile (see curve 1) does exhibit exponential tails, which localize the wave function to a small space volume. Then two identical layers of 82.5-μm thick (see curve 2) are added to this structure on both sides and the resulting field profile is calculated for the whole composite sample of 330 μm (see curve 3, Fig. 6). It can be clearly seen from a comparison of curves 1 and 3 that the initial state completely retains its initial shape. This indicates that the state 1 ''feels'' its environment only through exponential tails and is relatively insensitive to the background beyond the localization length, which can be defined now as an exponent in the tail region of the profiles for a single realization of disorder (about 8 μm for curve 1).

To obtain complete localization in this sense in a 3D structure, it is necessary to create analogous localized states at the same frequency for all other directions (and polarizations), which spatially overlap. This can be achieved in a disordered 3D photonic crystal with gaps for different directions, which are energetically overlapping. This condition is also very similar to that for opening up a complete PBG, except that the widths of the perturbed gaps can be significantly larger in a disordered crystal, thus facilitating spatial localization.

VI. DISCUSSION

Analysis of different localization regimes presented above allow us to argue that the experimentally observed broadening and smoothing of the photonic gap in opals is induced by intrinsic disordering of their photonic lattice and can be ascribed to building up of the second regime of localization. The smooth transmission curves appear in experiment because ensemble averaging is already performed by probing the huge volume of the sample (surface area defined by the diameter of the probe beam times the sample thickness is about 10^6 μm^3 or 10^8 unit cells). However, it becomes clear from the above discussion that photon transport through the opal sample is mediated by photonic states, like that presented in Fig. 6, strongly localized at least in the direction of incidence. These states can be responsible for recently observed large enhancement of optical gain in opals at the frequencies of a photonic gap.[12] Recently reported decrease of the decay time of dye molecules impregnated in the opal structure[27] can be also explained by the enhancement of a local-field amplitude of the localized states characterized by a high-Q value.

Note that experimental values of attenuation length can be well fitted only with assumption of a very large disorder δ of more than 30%. Bearing in mind that all kinds of disorder are equivalent in terms of accumulation of a phase shift of transmitting wave, it can be concluded that, except for the disorder associated with deviation in spheres diameter, a large concentration of other types of defects is presented in the sample. The presence of in-plane disorder and, especially, the stacking faults along (111) planes, which was shown to be the main structural defects in opal lattices,[10,13] helps to localize the wave function also in the directions perpendicular to [111]. Even for samples with relatively small concentration of stacking faults, the gaps in directions perpendicular to the [111] direction of growth are very broad and overlap with each other and also with the [111] gap.[10,13] This implies the nonzero probability of finding such a state within the sample volume, which is strongly localized in all three dimensions.

VII. CONCLUSION

In conclusion, two different regimes of light localization in a disordered photonic crystal are identified, which build up consequently depending on the amount of disorder compared with the normalized width of the gap in corresponding periodic structure. This comparison can be applied to gaps for different directions and therefore it remains valid for the photonic crystal of any dimensionality. Indeed, for extending of our findings to three-dimensional photonic band-gap crystal one should operate with the term ''complete photonic band gap'' instead of ''gap for specific direction.'' Then the local fluctuations of the photonic band edges, now of a complete band gap, caused by random disorder should be compared with the width of a complete photonic band gap. Thus we arrive to the same conclusion—there exist several qualitatively different regimes of light localization in a three-dimensional case also.

The analysis performed allows us to describe the experimentally observed situation in opal photonic crystal as the building up of the second regime of light localization. It should be noted that an increase of the refractive index contrast in opal photonic lattices (which can be provided, for example, by the filling of the interstitials by a high refractive index material[11,15–17]) leads to increase of the gap width, which can result in the appearance of the first regime of strong light localization.

Note added in proof. We recently became aware of a similar approach, which allows one to distinguish between two different modes of localization in a 1D periodic-on-average system.[28] Based on Monte Carlo calculations of the statistics of the Lyapunov coefficient ξ^{-1}, it was shown that an increase of the degree of randomness δ beyond a well-defined critical value results in a transition from the anomalous dependence of the variance of var(ξ^{-1}) on ξ^{-} to the usual single parameter scaling behavior. Based on the results of our work we can argue that the transition between these

two regimes of scaling occurs when the local fluctuations of the band-edge frequency are larger than the gap width. Such interpretation gives a physical understanding of the effect.

ACKNOWLEDGMENTS

We would like to thank O. Z. Karimov for technical assistance in transmission measurements. Fruitful discussions with V. N. Astratov, A. A. Kaplyanskii, I. P. Ipatova, and E. L. Ivchenko are gratefully acknowledged. We are grateful to D. Cassagne for providing us with results of full-vector 3D calculations of the photonic band structure of opals. This work was supported in part by the RFBR, Grants No. 960217928 and 980218259.

APPENDIX: THE PROFILE OF DIELECTRIC FUNCTION ALONG THE [111] DIRECTION IN A fcc LATTICE COMPOSED OF SPHERES

We consider 3D fcc periodic photonic crystal of opal as a 1D layered structure, in which the refractive index depends only on one coordinate z. If z is chosen to be [111] direction of fcc lattice then a period of $n(z)$ is equal to the distance between two neighboring (111) layers of close-packed spheres $(2\sqrt{6}/3)\cdot R$, where R is a radius of the spheres. In order to obtain an analytic formula for the refractive index profile $n(z)$ [see Eq. (1)], it is necessary to calculate an expression for $S_{sp}(z)$, which is a relative area cross section of the spheres in a (111) plane calculated as a function of the distance along z direction. The latter is given by

$$S_{sp}=\frac{\pi}{2\sqrt{3}}\left(1-\frac{z^2}{R^2}\right), \quad \text{for } 0\leqslant z<\left(\frac{2\sqrt{6}}{3}-1\right)R, \tag{A1}$$

$$S_{sp}=\frac{\pi}{2}\left(\frac{4\sqrt{2}}{3}\frac{z}{R}-\frac{2}{3\sqrt{3}}-\frac{2}{\sqrt{3}}\frac{z^2}{R^2}\right)$$

$$\text{for } \left(\frac{2\sqrt{6}}{3}-1\right)R\leqslant z<R, \tag{A2}$$

$$S_{sp}=\frac{\pi}{2}\left(\frac{4\sqrt{2}}{3}\frac{z}{R}-\frac{5}{3\sqrt{3}}-\frac{1}{\sqrt{3}}\frac{z^2}{R^2}\right), \quad \text{for } R<z\leqslant\frac{2\sqrt{6}}{3}R. \tag{A3}$$

The coordinate z is chosen to be zero in the center of a sphere. Equations (A1) and (A3) correspond to the case when a cross section passes through the center of the spheres belonging to a single layer. The spheres from two neighboring layers give contribution to a resulting cross section in the case of Eq. (A2). The profile calculated according to Eqs. (A1)–(A3) and Eq. (1) is shown in the inset of Fig. 4.

*Present address: NEC Research Institute, 4 Independence Way, Princeton, NJ 08540. URL: www.neci.nj.nec.com/homepages/vlasov

†Also at Department of Physics, University of Durham, South Road, Durham DH1 3LE,U.K.

[1] See, for example, P. Sheng, *Introduction to Wave Scattering, Localization, and Mesoscopic Phenomena* (Academic, San Diego, 1995).

[2] N. Garcia and A. Z. Genack, Phys. Rev. Lett. **66**, 1850 (1991); A. Z. Genack and N. Garcia, *ibid.* **66**, 2064 (1991); A. Z. Genack, *ibid.* **58**, 2043 (1987).

[3] Y. Kuga and A. Ishimaru, J. Opt. Soc. Am. A **1**, 831 (1984); M. P. Van Albada and A. Lagendijk, Phys. Rev. Lett. **55**, 2692 (1985).

[4] D. S. Wiersma, P. Bartolini, A. Lagendijk, and R. Righini, Nature (London) **390**, 671 (1997).

[5] A. F. Ioffe and A. R. Regel, Prog. Semicond. **4**, 237 (1960).

[6] S. John, Phys. Rev. Lett. **58**, 2486 (1987).

[7] For a review, see articles in *Photonic Band Gap Materials*, Vol. 315 of *NATO Advanced Study Institute, Series E: Applied Sciences*, edited by C. M. Soukoulis (Kluwer, Dordrecht, 1996).

[8] M. Stoytchev and A. Z. Genack, Phys. Rev. B **55**, 8617 (1997).

[9] V. N. Astratov, V. N. Bogomolov, A. A. Kaplyanskii, A. V. Prokofiev, L. A. Samoilovich, S. M. Samoilovich, and Yu. A. Vlasov, Nuovo Cimento D **17**, 1349 (1995).

[10] V. N. Astratov, Yu. A. Vlasov, O. Z. Karimov, A. A. Kaplyanskii, Yu. G. Musikhin, N. A. Bert, V. N. Bogomolov, and A. V. Prokofiev, Phys. Lett. A **222**, 349 (1996).

[11] Yu. A. Vlasov, V. N. Astratov, O. Z. Karimov, A. A. Kaplyanskii, V. N. Bogomolov, and A. V. Prokofiev, Phys. Rev. B **55**, 13 357 (1997).

[12] Yu. A. Vlasov, K. Luterova, I. Pelant, B. Hönerlage, and V. N. Astratov, Appl. Phys. Lett. **71**, 1616 (1997).

[13] Yu. A. Vlasov, V. N. Astratov, A. V. Baryshev, A. A. Kaplyanskii, O. Z. Karimov, and M. F. Limonov (unpublished).

[14] K. Busch and S. John, Phys. Rev. E **58**, 3896 (1998).

[15] J. Wijnhoven and W. L. Vos, Science **281**, 802 (1998).

[16] A. A. Zakhidov, R. H. Baughman, Z. Iqbal, C. Cui, I. Khairulin, S. O. Dantas, J. Marti, and V. G. Ralchenko, Science **282**, 897 (1998).

[17] Yu. A. Vlasov, N. Yao, and D. J. Norris, Adv. Mater. **11**, 165 (1999).

[18] Yu. A. Vlasov, S. Petit, G. Klein, B. Hönerlage, and Ch. Hirlimann, Phys. Rev. E **60**, 1030 (1999).

[19] W. Stöber, A. Fink, and E. Bohn, J. Colloid Interface Sci. **26**, 62 (1968).

[20] R. Graag, R. K. Prud'homme, I. A. Aksay, F. Liu, and R. R. Alfano, J. Opt. Soc. Am. A **15**, 932 (1998).

[21] J. M. Frigerio, J. Rivory, and P. Sheng, Opt. Commun. **98**, 231 (1993).

[22] A. R. McGurn, K. T. Christensen, F. M. Mueller, and A. A. Maradudin, Phys. Rev. B **47**, 13 120 (1993).

[23] V. D. Freilikher, B. A. Liansky, I. V. Yurkevich, A. A. Maradudin, and A. R. McGurn, Phys. Rev. E **51**, 6301 (1995).

[24] D. Cassagne (private communication).

[25] See, for example, I. P. Ipatova, in *Optical Properties of Mixed Crystals*, edited by R. J. Elliot and I. P. Ipatova (Elsevier, New York, 1988).

[26] D. J. Thouless, Phys. Rep., Phys. Lett. **13C**, 93 (1974).

[27] E. P. Petrov, V. N. Bogomolov, I. I. Kalosha, and S. V. Gaponenko, Phys. Rev. Lett. **81**, 77 (1998).

[28] L. I. Deych, D. Zaslavsky, and A. A. Lisyansky, Phys. Rev. Lett. **81**, 5390 (1998).